

A&A manuscript no.
(will be inserted by hand later)

Your thesaurus codes are:
06 (08.16.4; 08.05.3; 08.13.2)

Full spectrum of turbulence convective mixing: II. Lithium production in AGB stars.

I. Mazzitelli¹ F. D’Antona² and P. Ventura²

Osservatorio Astronomico di Roma, Monte Porzio Catone, I-00040 (Rome)
email: paolo@coma.mporzio.astro.it

Received 23 february 1999; accepted ???????

Abstract. We present results from new, detailed computations of lithium production by hot bottom burning (HBB) in asymptotic giant branch (AGB) stars of intermediate mass ($3.5 \leq M \leq 6M_{\odot}$). The dependence of lithium production on stellar mass, metallicity, mass loss rate, convection and overshooting are discussed. In particular, nuclear burning, turbulent mixing and convective overshooting (if any) are self-consistently coupled by a diffusive **algorithm**, and the Full Spectrum of Turbulence (FST) model of convection is adopted, with test comparisons to Mixing Length Theory (MLT) stellar models. All the evolutions are followed from pre-main sequence down to late AGB, when stars do not appear any longer lithium rich. A “reference mass” of $6 M_{\odot}$ has been chosen since, although relatively close to the upper limit for which degenerate ^{12}C ignition occurs, all the studied mechanisms show up more clearly.

HBB is always found above $\sim \log L/L_{\odot} = 4.4$, but the range of (initial) masses reaching HBB is largely dependent on convection model, overshooting and metallicity. For solar chemistry, masses $\geq 4M_{\odot}$ evolve through HBB in the FST case and including core overshooting whereas, with solarly tuned MLT models and no overshooting, only masses $\geq 6M_{\odot}$ can reach HBB. These constraints can give feedbacks about the more correct convection model and/or the extent of overshooting, thanks to the signatures of HBB in AGB stars in clusters of known turnoff masses and metallicity.

Overshooting (when included) is addressed as an exponentially decreasing diffusion *above* formally convective regions. It makes convective cores during the main sequence to grow larger, and also starting masses and luminosities in AGB are then larger. However, also preliminary results obtained when allowing displacement of convective elements *below* convective regions in AGB are shown. In the “reference” case ($6M_{\odot}$), we find that overshooting from below the convective envelope *totally suppresses thermal pulses* and ultimately leads to the formation of massive ($\sim 1M_{\odot}$) white dwarfs rich in Carbon and Oxygen immediately below the photosphere.

Key words: stars: evolution of – AGB and post AGB – mass loss

1. Introduction

Lithium has been always the subject of extensive investigations, mainly due to its cosmological importance. The hottest (and most massive) among the population II main sequence stars display a plateau in the lithium abundance (Spite & Spite 1993), clustering around $\log \epsilon(^7\text{Li}) = 2.24 \pm 0.012$ (Bonifacio & Molaro 1997), where $\log \epsilon(^7\text{Li}) = \log(^7\text{Li}/H) + 12$. Stars in young open clusters (Pleiades, Praesepe etc.) display an analogous plateau, with an abundance roughly a factor of ten larger (Soderblom et al. 1990, 1993a,b, Balachandran et al. 1988, 1996). A *bona fide* (and Ockham-like) explanation of this dichotomy would require the existence of stars producing and recycling lithium in the interstellar medium. The discovery of a few tens of lithium rich AGB stars in the Magellanic Clouds (Smith & Lambert 1989,1990), with $\log \epsilon(^7\text{Li})$ up to ~ 3.8 , strongly recommends to take into account massive AGB stars as possible candidates (D’Antona & Matteucci 1991), although they might not be the only indicted (Matteucci et al. 1995).

A mechanism for lithium production in stars has been suggested by Cameron & Fowler (1971) who hypothesized that, if the temperature at the base of the envelope of an AGB star is $T_{bce} \geq 4 \cdot 10^7\text{K}$, “Hot Bottom Burning” with enhanced production of ^7Be will **occur**. This latter element, if fastly carried away by convection from high-T regions, might decay into lithium in the outermost envelope of the star.

Static envelope models have been used to describe in a first approximation the above mechanism, both by Sackmann et al. 1974 and Scalo et al. 1975. More recently, Sackmann & Boothroyd (1992) built up evolutive stellar models through the thermal pulse (TP) phase, also testing the effect of mass loss and metallicity. Li-production in intermediate mass stars was found within an MLT framework, when tuning $\alpha = l/H_p > 2$. However, the present MLT tuning of the solar model –with updated physical

Table 1. Inputs for the computed models

M	Start	Conv.	ζ	\dot{M} (η)	Z	M_c/M_\odot^a
6	PMS	FST	0	0	0.02	0.931
6	$D = 10^{-5}$	FST	0	0	0.02	0.929
6	MS	FST	0	0	0.02	0.931
6	PMS	MLT	0	0	0.02	0.931
5	PMS	FST	0	0.1	0.02	0.925
5	PMS	FST	0	0.05	0.02	0.925
6	PMS	FST	0	0	0.01	0.945
6	PMS	FST	0	0	0.001	0.988
6	PMS	FST	0	0.3	0.02	0.922
6	PMS	FST	0.02	0.1	0.02	0.98 ^b
			(symm)			
6	PMS	FST	0.02	0.1	0.02	1.013
5.5	PMS	FST	0.02	0.1	0.02	0.962
5	PMS	FST	0.02	0.1	0.02	0.925
4.5	PMS	FST	0.02	0.1	0.02	0.874
4	PMS	FST	0.02	0.1	0.02	0.812
3.5	PMS	FST	0.02	0.1	0.02	0.665

^a Value of the core masses refer to the interpulse phase between the fifth and the sixth pulse.

^b Core mass at the end of computation.

inputs– ranges between $\alpha \sim 1.5 \div 1.7$; with these low values of α the onset of HBB is shifted to larger initial masses. Of course, nobody claims that the solar tuning of α must rank as a universal constant, but the above findings strongly recommend to test more updated and less tuning dependent convective models.

Exploration of HBB phases according to a more modern treatment of turbulent convection (D’Antona & Mazzitelli 1996) started after the availability of the FST model by (Canuto & Mazzitelli 1991,1992). HBB in solar metallicity stars of intermediate mass was found to be a straightforward and tuning-independent consequence of use of the FST model. In the present follow-up of the ’96 work, the version of the ATON code (**ATON 2.0**, Ventura et al. 1998) has been implemented with a diffusive algorithm for chemical evolution which can fully address the problem of lithium production in AGB stars. We delay to a following paper the tuning of overshooting and mass loss required to fit the observations of AGB Lithium rich stars in the Magellanic Clouds. Here we test the role of different input parameters.

Our standard model will be a $6M_\odot$, $Z = Z_\odot = 0.02$, with an initial D -abundance (by mass) $X(D) = 2 \cdot 10^{-5}$. We investigate the effects of different convection models, initial deuterium abundances, metallicity, overshooting, mass loss rate and initial stellar mass on the AGB phase. Mainly, we focus our attention on the core mass versus luminosity relation, on the amount of lithium produced, and on the duration of the phase during which the star can be seen as lithium rich. Figure 1 shows the HR diagram

Fig. 1. HR diagram of 3.5, 4, 4.5, 5, 5.5 and $6M_\odot$ models of solar chemistry evolved from the pre-main sequence to the first thermal pulses.

of the main computed set of tracks from $3.5M_\odot$ to $6M_\odot$. The tracks shown include mass loss and core overshooting. The Thermal Pulse phase, shown only for the masses 4, 5 and $6M_\odot$, appears as a series of loops in the diagram at luminosities between $\log L/L_\odot \simeq 4.4$ and 4.8.

2. Stellar modelling

The main features of the **ATON 2.0** code are described in details in Ventura et al. (1998). In this paper we re-discuss the coupling between nuclear and turbulent chemical evolution (2.1). We also briefly recall the main micro/macrophysical inputs:

- Radiative opacities from Rogers & Iglesias (1993), and from Alexander & Ferguson (1994) for the low-temperature regime;
- neutrino losses from Itoh et al. (1992);
- electron conduction from Itoh & Kohyama (1993);
- OPAL EOS (Rogers et al. 1996) for $3.7 < \log T < 8.7$ is adopted. In the low-T – high- ρ limit, the Mihalas et al. (1988) EOS is also included;
- the nuclear network explicitly accounts for the 14 elements: 1H , 2D , 3He , 4He , 7Li , 7Be , ^{12}C , ^{13}C , ^{14}N , ^{15}N , ^{16}O , ^{17}O , ^{18}O , ^{22}Ne . 22 reactions are considered, from the light elements burning up to ^{12}C ignition. Cross-sections are taken from Caughlan & Fowler (1988) and screening factors by Graboske et al. (1973). Although in HBB very large temperatures can be met in the H-burning shell, we omitted the Na–Al cycle since its contribution to the total energy generation is always negligible. More about this subject in the following;
- the size of convective regions is evaluated according to the Schwarzschild criterion. The convective fluxes can be computed either by the FST model (Canuto et al. 1996, updating the Kolmogorov constant to 1.7), or by the MLT (Vitense 1953). In these latter models, we use our solar tuning of the free parameter $\alpha = 1/H_p = 1.55$.

2.1. Chemical evolution and overshooting

Instead of addressing chemical mixing inside convective regions within the instantaneous mixing approximation, we adopt the more physically sound full-coupling between nuclear evolution and turbulent diffusion (see Ventura et al. 1998). This is necessary both to follow lithium production/destruction, and to allow for a self-consistent treatment of diffusive overshooting in conditions when leakage of an high-T CNO-burning shell is present. Let us discuss this latter point.

In HBB conditions, even in the absence of overshooting from *below* the convective envelope, convection penetrates the H-burning shell such that a non negligible fraction ($\sim 20 \div 30\%$) of the star’s luminosity is generated inside a turbulently mixed region (see later). Of course, this effect is increased if we allow for some amount of overshooting.

Our results show that the following two problems arise:

- the nuclear time scales of some CNO reactions can become of the same order of magnitude of the convective time scales, and
- the local H/He production/destruction can be *relatively* large during one single time step.

The solution of the second problem necessarily leads to the requirement of using a larger-than-zero order for the numerical integration of the nuclear evolution. We adopt the scheme by Arnett & Truran (1969) which, being an implicit, first order treatment, gives integration errors $\propto (\delta X)^2$ instead of $\propto (\delta X)$ (remember that $\delta X \ll 1$).

The above procedure requires however the explicitation of *all* the chemical abundances not only *before*, but also *after* the time step, including the effect of mixing. So, if we want to account also for the first problem above (similarity of time scales), no semi-explicit solution, point by point and element by element along the structure (as for instance in Herwig et al. 1997) is allowed. The only fully self-consistent solution is to store *all the matrix elements along the whole structure*, and invert the general matrix. This is a burdensome task, and also explains why we limit to 14 elements our network. Our chemical evolution scheme is however more physically sound (actually: the only physically sound one) than any other used up today, if extreme cases of HBB are to be considered.

As for overshooting, in our code we can follow two distinct approaches:

- In case of tests with the oversimplified approximation of instantaneous mixing, we simply force full mixing up to a fixed distance from the formal convective border. The extent of the overshooting region, usually taken as a fraction of H_p , is a free parameter.
- In case of diffusive mixing, we use the formalism described by Ventura et al. (1998), allowing an exponential decay of the convective velocity out of any convective border of the form:

$$u = u_b \cdot \exp\left(\frac{1}{\zeta f_{thick}} \ln \frac{P}{P_b}\right), \quad (1)$$

where u_b and P_b are turbulent velocity and total pressure at the convective boundary, P is the local pressure, ζ is a free parameter.

Our treatment of diffusive overshooting is then not far different from that adopted by Herwig et al. (1997). We prefer to use pressure instead of distance to compute exponential decay, since the first non-local models by Xiong

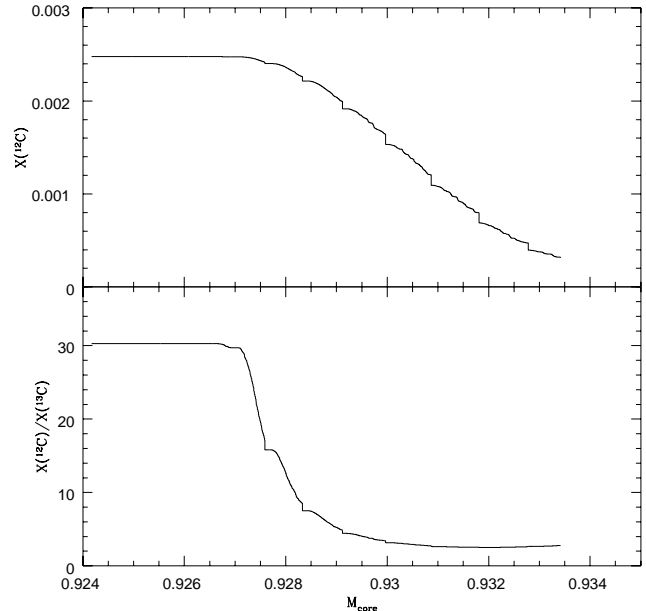


Fig. 2. Variation with core mass of ^{12}C surface abundance (**top**) and of the ratio $^{12}\text{C}/^{13}\text{C}$ (**bottom**) within the “standard” $6M_{\odot}$ model. The rapid drop of $^{12}\text{C}/^{13}\text{C}$ is a clear evidence of HBB at the base of the convective envelope.

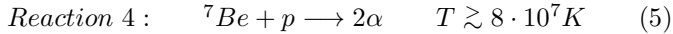
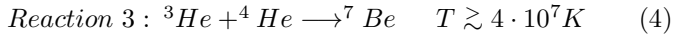
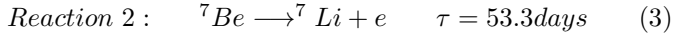
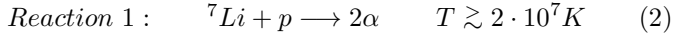
(1985) suggest pressure as the more correct choice, but until overshooting occurs along short scales, pressure and distance are almost linear with each other. The main difference is rather that Herwig et al. (1997) use MLT convective velocities and scale lengths to evaluate the diffusive coefficient. While FST and MLT turbulent velocities turn out to be quite similar, it is not so for the scale lengths, especially close to the convective boundaries (and then also close to the CNO-burning shell), where the MLT can overestimate the local scale length by more than one order of magnitude.

The free parameter ζ is a measure of the size of the overshooting region; lower ζ ’s allow a steeper decay of velocity and a narrower overshooting region. Qualitatively, it is similar Herwig et al.’s free parameter f . The quantity f_{thick} in eq.1 is the thickness of the convective region in fractions of H_p (up to a maximum of 1), scaling the overshooting distance according to the width of the convective zone.

The tuning of ζ has been performed by Ventura et al. (1998). For main sequence stars of any mass (including the solar one), $\zeta = 0.02$ gives results consistent with the analysis of open clusters HR diagrams by Maeder & Meynet (1991) and Stothers & Chin (1992). We therefore assume that, at least in a first approximation, the above tuning of ζ be representative of the overall characteristics of overshooting, at least from the top of a deep convective region.

Fig. 3. Left: Variation with core mass of the luminosity (**top**) and temperature at the base of the convective envelope (**Bottom**) for our standard model of $6M_{\odot}$ (full lines) and for the corresponding track assuming the MLT model for turbulent convection. The FST model leads to larger temperatures, thus favouring lithium production. **Right:** Variation with core mass of the surface lithium within a $6M_{\odot}$ with two different models for turbulent convection. **Bottom:** Variation with core mass of ${}^3\text{He}$ surface abundance. We note that in the MLT case the ${}^3\text{He}$ depletion remains negligible despite lithium production.

As for lithium production/destruction, the main reactions are listed below, together with the temperature at which they become important in HBB conditions.



Note that the temperatures are \sim one order of magnitude larger than those at which the same reactions are active in previous evolutionary phases. This is due to the very short time scale of the whole AGB phase, requiring extremely large reaction rates to lead to appreciable chemical evolution.

Let us shortly resume the Li-production mechanism. Lithium is destroyed very quickly due to proton capture (reaction 1), and the only production channel is via Beryllium decay on the timescale τ of reaction 2. In turn, ${}^7\text{Be}$ is produced through reaction 3 and, at large temperatures, it can be also destroyed by a proton capture (reaction 4).

The problem in getting lithium production stems from the facts that lithium is immediately destroyed via reaction (1), and that also the ignition of reaction (4) could prevent beryllium from decaying into lithium. The solution suggested by Cameron & Fowler (1971) is based on two facts:

- for temperatures $T < 8 \cdot 10^7 \text{K}$, the rate of reaction (4) is not so large to prevent beryllium decay: moreover, reaction (4) is slower than mixing at the base of the convective envelope;
- inside the very expanded envelope of AGB stars, beryllium decay is slow enough that lithium production occurs in cooler regions of the envelope of the star, where it can survive to show up at the surface.

In this scheme, nuclear evolution and mixing are so strictly intertwined that they cannot be dealt within the instantaneous mixing approximation. Surface lithium would be in fact mixed at once, to be instantaneously destroyed at the base of the envelope.

Of course, the solution by Cameron & Fowler (1971) can work if reaction (4) is not running too fast at the base of the external envelope (Sackmann & Boothroyd 1992, 1995), otherwise proton capture would leave no beryllium available to decay into lithium. Computations show that, for $T < 8 \cdot 10^7$ reaction (4) is slower than mixing and overabundances of lithium can be observed. If HBB occurs

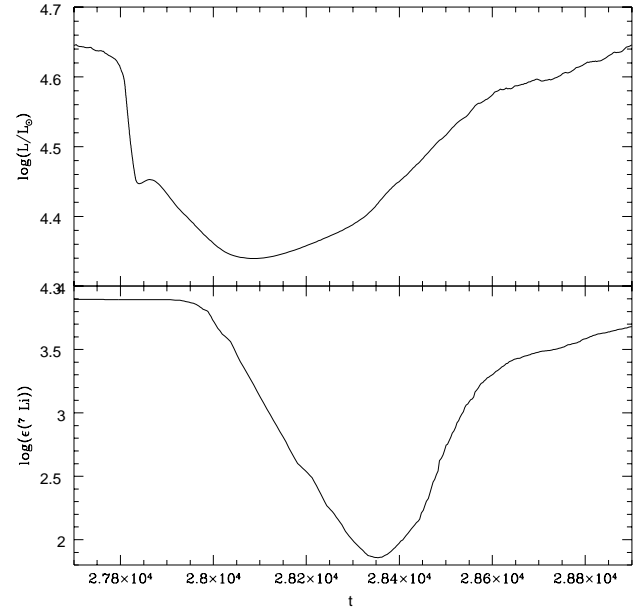


Fig. 4. Variation of luminosity and surface lithium abundance during a thermal pulse. Times were normalized to the 2nd dredge – up. We note a temporal delay between lithium depletion with respect to the drop in luminosity, which is due to the time needed by convection to carry matter depleted in lithium at the surface of the star.

at larger temperatures, beryllium burns at the base of the envelope, and lithium in the envelope begins to decrease.

3. Evolution of a $6M_{\odot}$ star

We first discuss, for reference, the evolution of a $6M_{\odot}$ model starting from the pre-main sequence (PMS), with no mass loss, no overshooting and FST convection. The chemistry is solar ($Y = 0.28, Z = 0.02$), and initial deuterium and lithium abundances (in mass) of respectively $2 \cdot 10^{-5}$ and $2 \cdot 10^{-8}$ ($\log \epsilon({}^7\text{Li}) = 3.6$) are assumed. The track has been followed until the star underwent a handful of Thermal Pulses (TPs). We shortly elucidate the surface chemical evolution, mainly of ${}^3\text{He}$ and ${}^7\text{Li}$, prior to the beginning of the AGB phase. Remember that ${}^3\text{He}$ is a key ingredient (reaction 4) in ${}^7\text{Li}$ -production.

During PMS, D-burning leads to an ${}^3\text{He}$ abundance of $3 \cdot 10^{-5}$ in a large fraction of the structure. Lithium depletion is large in the interior, but negligible at the sur-

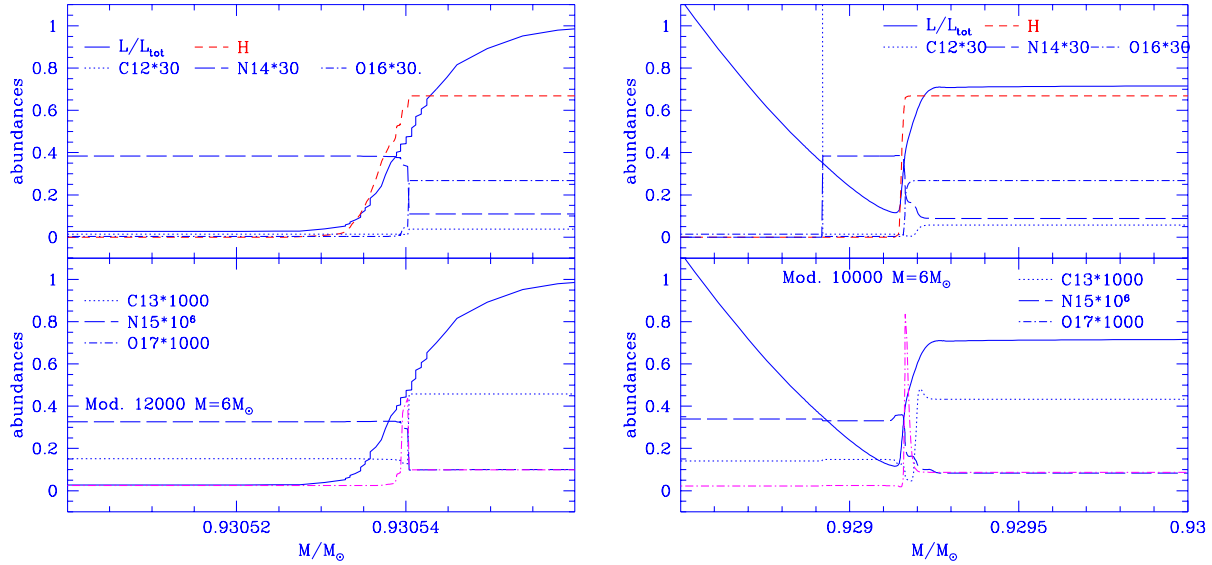


Fig. 5. Chemical profiles in the *convective* hydrogen burning shell are shown for standard models without overshooting in two different phases. Model 12000 (left) is during stationary H–burning; model 10000 (right) during a TP. In the interpulse phase, $\sim 30\%$ of the nuclear luminosity is born in the lower part of the convective envelope; correct coupling between nuclear evolution and turbulent mixing is then necessary to account for the CNO equilibria and the energy output.

face, since the temperature at the bottom of the (thin) convective envelope is always $T_{bce} < 2 \cdot 10^6 \text{K}$.

A first drop in lithium abundance follows the first dredge up, when the base of the convective envelope reaches layers where lithium had been previously destroyed. At the end of this phase, $\log \epsilon(^7\text{Li}) = 2.1$ and the ^3He abundance increases up to $6 \cdot 10^{-5}$, due to the sinking of convection down to regions where incomplete $p-p$ burning occurred. Also ^4He increases up to 0.29, and the CNO isotopic abundances keep track of mixing up to the stellar surface of CNO processed matter.

At the second dredge up, following He–ignition in a thick shell around the C/O core and exhaustion of the H–burning shell, the ^4He abundance rises to 0.31, but no other important modifications in the isotopic abundances are found. The lithium surface abundances starts changing significantly soon after exhaustion of the thick He–burning shell and re–ignition of the H–shell, when the T_{bce} starts increasing and, as soon as this latter overcomes 10^7K , it drops to $\log \epsilon(^7\text{Li}) \sim 0.3$. Only when $T_{bce} \sim 3 \cdot 10^7 \text{K}$, the Cameron-Fowler mechanism begins to be efficient, and lithium production takes over lithium burning (Fig.2 and 3). This is also the phase when the first TPs are ignited. Since these latter are responsible for large excursions of temperature at the bottom of the convective envelope, they also affect lithium evolution, as detailed in the following.

The core mass in the TP phase is $\sim 0.93M_{\odot}$; lower than found in D’Antona & Mazzitelli (1996) mainly due to

the different evolutionary scheme, and in close agreement with Wagenhuber & Groenewegen (1998).

During the TP phase, $\log \epsilon(^7\text{Li})$ fastly increases up to a maximum value of ~ 3.8 soon after the second major pulse. It fastly drops shortly after the peak of each TP, due to the decrease of T_{bce} following the He–outburst, and then recovers its maximum abundance. Both drop and recovering are slightly delayed with respect to the answer of the surface of the star to TPs (fig.4), due to the relatively long time required by convection to fully mix the very expanded envelope.

Going ahead with the TPs, the plateau value of $\epsilon(^7\text{Li})$ begins to slowly decrease. This is due to the onset of two mechanisms:

- the temperature at the bottom of the convective envelope goes on increasing (Fig.3, bottom left panel) until reaction 4 begins to compete with reaction 2, and some ^7Be is no more available to produce ^7Li , and
- in the absence of reactions producing ^3He , this latter element begins to be consumed by reaction 4 (Fig.3, bottom right panel), and also ^7Be –production is no more very efficient.

Another mechanism worth discussing is the relatively large fraction of the H–burning shell interested by convection. From Fig.5 we see that a non negligible fraction of the nuclear luminosity is generated *inside* the convective envelope. This explains the very fast drop in the surface ^{12}C abundance, and the even faster reaching of the $^{12}\text{C}/^{13}\text{C}$

equilibrium ratio in a very few pulses (fig.2). Fig.5 shows the ^{15}N profile close to the bottom of the convective envelope, during an interpulse. Since ^{15}N is a bottleneck in the CNO cycle, any evolutive scheme other than full coupling between mixing and nuclear evolution is bound to fail in correctly describing the nuclear output in the convective fraction of the H-shell. This will be more and more relevant when also overshooting from *below* the envelope will be accounted for.

In conclusion, we find that a straightforward application of the FST model immediately and nicely leads to the occurrence of HBB in AGB of intermediate mass stars, and to the appearance of ^7Li overabundances, without requiring a non-solar tuning of the model itself. Let us then start discussing the results found when changing either the tuning of the FST model, or the convective model as a whole.

4. Influence of the convective model

The FST convective model allows for a limited amount of tuning thanks to the β parameter (for a complete discussion and for the solar tuning see Ventura et al. 1998). Since the standard evolution was computed with $\beta = 0.1$, we tested one more evolution with $\beta = 0.05$.

From a physical point of view, this latter choice leads to a shorter turbulent scale length close to the convective boundaries, making convection slightly less efficient. In AGB conditions, the final result is that the base of the envelope is, on the average, cooler. As a consequence, the Cameron-Fowler mechanism runs at a slower pace, and the amount of lithium produced is lower. However, some (small) differences are found only during the first three TPs, after which the plateau value of $\epsilon(^7\text{Li})$ becomes insensitive to the tuning of the FST model. We found only one clear difference between the two cases: at the peak of the TP, lithium destruction is larger the larger is β . This is, in our opinion, a negligible effect, since these phases are very short lived compared with the interpulse times. We then conclude that, at variance with what happens in the MLT case, lithium production in AGB is largely independent of tuning within the FST convective model.

As for the tests with the MLT, we first recall that D’Antona & Mazzitelli (1996) examined in detail the dependence of lithium production during the AGB phase on the convective model. In the case of a $5M_{\odot}$ star they found that, in the MLT case, HBB could be achieved only with a value of the free parameter $\alpha \sim 2.5$, consistent with Sackmann and Boothroyd 1992. When assuming the solar tuning $\alpha = 1.5$, no trace of ^3He depletion (see their Fig.4) for the first six pulses was found (full coupling between nuclear and turbulent evolution was not yet implemented in the code), leading the authors to conclude that no significant lithium production might be accomplished in that case. Here we examine the case of a $6M_{\odot}$, for which we

follow the evolution with MLT and the present solar tuning $\alpha = 1.55$.

The results are shown in Fig.3 where we report the evolution vs. core mass of surface luminosity, T_{bce} , $\epsilon(^7\text{Li})$ and $X(^3\text{He})$ in the FST (standard) and MLT sequences. First note that, before the onset of the TPs, the two tracks show quite different surface lithium abundances, the MLT models maintaining ~ 100 times more ^7Li than the FST one.

A relevant result is that the core mass – luminosity relation is largely affected by the convection model. At core mass $0.93M_{\odot}$, FST models are ~ 2 times more luminous than MLT ones. This is due to the intrinsically lower efficiency of the MLT convection with respect to the FST one, and we have already seen that the lower is the efficiency, the lower is T_{bce} . Since the temperature in the H-burning shell is quite close to T_{bce} (there is a merge between convective envelope and shell), solarly tuned MLT models are cooler and less luminous, and can be made consistent with FST ones only at the price of artificially enhancing the convective efficiency by increasing α .

At the same time, the lower T_{bce} in the MLT case makes the Cameron-Fowler mechanism less efficient and, in fact, MLT ^7Li -production takes longer (~ 10 TPs) before being comparable to the FST one. Also ^3He begins to be depleted, in the MLT case, only after a number of pulses, when ^7Li approaches the maximum, while in the FST case it starts decreasing at the first pulses.

We did not repeat the computations with larger values of α , since the present models are largely consistent with those by D’Antona & Mazzitelli (1996). The preliminary conclusion which can be drawn by the above results is then that also MLT models with solarly tuned α can give rise to Li-rich AGB’s, but the range of initial masses undergoing HBB is very narrow; below $6M_{\odot}$ no Li-enhancement can be obtained, and already at $6.5 \div 7.0M_{\odot}$ degenerate ^{12}C ignition in the core stops evolution before the onset of TPs. In the FST case, as we will see later, already stars of $4.0 \div 4.5M_{\odot}$ can attain HBB.

These conclusions will be later strengthened, when discussing the occurrence of (possible) overshooting from the core, and (unavoidable) mass loss. As we will show, the chances are that these stars undergo a relatively low number of TPs before planetary nebula ejection. Little or no Li-enrichment of the interstellar medium is then expected if the Cameron-Fowler mechanism does not **occur** very early in AGB.

5. Overshooting ”from above”

A small amount of convective overshooting at least from the core, both in MS and during the central He-burning phase, is likely to **occur** during the evolution of intermediate mass stars. In Ventura et al. (1998), the diffusive scheme here adopted to account for overshooting has been tuned as discussed in Sect. 2.1.

Fig. 6. Comparison between the standard $6M_{\odot}$ evolution (dotted line) and the model including core overshooting and mass loss (solid line). Overshooting leads to a larger core mass and faster evolution.

More disputable is the existence of overshooting from *below* a convective region. The helioseismological results by Basu (1997) severely constrain the amplitude of the region below the solar convective envelope, in which the temperature gradient is adiabatic. However, since non-local computations (Xiong 1985) show that the overshooting gradient sticks to the radiative one, we still get no informations about the amplitude of the *chemically mixed* region (if any), below a convective shell.

For this reason, we separated the two cases: overshooting *from above* a convective region, and *symmetric* overshooting. In the first case, discussed here, diffusive overshooting (fully coupled to nuclear evolution) is allowed from the top of *any* convective region, including the convective He–C shell at the peak of a TP, with the same tuning $\zeta = 0.02$. In the second case, discussed in a later section, the same tuning is applied to overshooting also from *below* any convective shell, including the external envelope and the He–C shell at the TP. In the following of this section, then, we will implicitly assume that overshooting occurs only from the top of *any* convective zone.

The main difference found with respect to the reference case (no overshooting) is the increased size of the H–exhausted core at the end of the MS phase. In fact, during central He–burning, the larger opacities of C and O lead to a “semiconvective–like” condition largely resetting the effect of a small amount of overshooting. Lastly, during TPs, the entropy barrier is large enough that even overshooting from the top of the He–C rich shell does not lead to mixing with the external H–rich layers.

At the end of the second dredge–up phase, then, the H–exhausted core mass is larger than without overshooting by $\sim 0.08M_{\odot}$, that is: $\sim 1.01M_{\odot}$. This is to be compared to the $\sim 1.05M_{\odot}$ required, in this phase, to ignite $^{12}\text{C} + ^{12}\text{C}$ degenerate burning off–centre, leading to sudden stop of the AGB (and to the birth of an O–Ne–Mg–rich WD?). If we define M_{up} as the initial stellar mass for which no AGB evolution occurs, even a small amount of overshooting in MS leads to $M_{up} \sim 6.5M_{\odot}$.

The $6.0M_{\odot}$ star, however, can still proceed through the TP phase. The larger core mass leads to a faster increase of T_{bce} than in the reference case, as soon as the H–burning shell is re–ignited. HBB takes over even prior to the ignition of TPs, and the surface lithium abundance reaches a maximum value $\log \epsilon(^7\text{Li}) \sim 4.1$. Also the $^{12}\text{C}/^{13}\text{C}$ surface ratio fastly drops to the equilibrium value.

These latter features are to be kept into account when comparing theory with observations. In *any* MLT environment, irrespective of the tuning of α , it is in fact very hard (overshooting or not) to get HBB with the corresponding surface chemical signatures before the igni-

tion of TPs. If, as expected according to the observations of relatively low–luminosity C–stars, the third dredge–up mechanism begins occurring already at the first TPs, s–process elements should almost always accompany Li–overabundances, as it happens in the Magellanic Cloud stars (Smith et al. 1995). If HBB takes over prior to the ignition of TPs, as in the present case, we can certainly expect to observe Li–overabundances without signature of s–process elements, as it has been recently found in a sample of galactic massive AGBs by Garcia Lario et al. (1998).

Of course, this result is insufficient to discriminate between convective models for the simple reason that, although we *reasonably* expect third dredge–up to immediately follow the onset of the TP phase, no convincing theoretical models still exist showing that this is indeed the occurrence, and, further, the lack of s–process enhancement in Garcia Lario et al. sample may have several other convincing explanations (see later). We only want to stress that, with FTP convection and a small (almost unavoidable, perhaps) amount of overshooting in MS, we spontaneously find Li–overabundances at the beginning of the AGB, prior to the ignition of TPs.

In Fig.6 we compare luminosity, T_{bce} and lithium evolution in the reference model and in a model with overshooting and mass loss (see next section for this latter mechanism). We see a fast decrease of the surface luminosity after $\sim 10^4\text{yr}$ from the second dredge up, due to the large mass loss rate adopted. Further, the evolution is faster, consistent with the higher core mass, and T_{bce} and lithium are larger, with respect to the no–overshooting case.

6. Mass loss

Mass loss in AGB is another physical feature to be obviously accounted for. Among the various possible choices, we decided to follow Blöcker’s (1995) recipe, to assume a Reimers’ rate:

$$\dot{M}_R = 4 \cdot 10^{-13} \eta \cdot \frac{LR}{M} \quad (6)$$

until the Mira oscillation period is lower than ~ 100 days, to switch to a much larger rate:

$$\dot{M} = \dot{M}_R \cdot L^{2.7} / M^{2.1} \quad (7)$$

when in AGB. The semiempirical tuning of the free parameter η according to Blöcker’s models is around 0.1, and we adopted the same value. However, Blöcker’s (1995) core masses in AGB are among the lowest available in the literature (Wagenhuber & Groenevegen 1998). Also his

Fig. 7. Variation with time of ${}^7\text{Li}$, luminosity, T_{bce} within two $5M_{\odot}$ models computed by assuming two different mass loss rates ($\eta = 0.1$ and $\eta = 0.05$). We note that increasing \dot{M} leads to a more rapid decrease of the luminosity of the star.

Fig. 8. Comparison between the $6M_{\odot}$ evolution without mass loss (track at the left) and the same evolution including mass loss with $\eta = 0.3$.

luminosities are then lower than the present ones for the same initial masses and evolutionary phases, and the stiff dependence of \dot{M} on L makes our *initial* mass loss rates in AGB $\sim 5 \div 10$ times larger than due. This is not yet relevant for the purposes of the present paper, since we are here interested in semi-quantitative comparisons only. We made some test computation on a $5M_{\odot}$ track, computing it with $\eta = 0.1$ and with $\eta = 0.05$. The comparison of the results is shown in Fig.7: the lower mass loss rate leads to a longer run of TPs, and the lithium abundance at the surface remains large for the whole run. In general, we can say that extensive computation of grids of evolutionary tracks will require values of η smaller than 0.1 for our models. Even more so, if overshooting (and corresponding increase of core mass and luminosity) is considered. The following discussion will however show that there is no linear relation between the value of η and the various evolutionary occurrences.

Mass loss dramatically modifies the evolution of our models. For the $6M_{\odot}$ case, after a few (~ 5) pulses the envelope mass decreases below $1M_{\odot}$, stopping HBB. After one–two further pulses, planetary nebula ejection should be expected. The duration of the lithium-rich phase is consistently reduced, the more the larger is the initial mass of the star. The effect is then relevant also to correctly determine the IMF of lithium-rich AGB stars.

Another feature to be stressed is that mass loss leads to early deviations from any core mass–luminosity relation. In fact, surface luminosity starts decreasing very soon. This affects the appearance of lithium rich stars in the HR diagram, since the same Li-abundance one would have found with no mass loss is now achieved at a lower luminosity. This is shown in Fig.8 where the AGB evolution of the $6M_{\odot}$ track without mass loss and with $\eta = 0.3$ are compared.

There is however another relevant consequence of the effect of mass loss on surface luminosity. It acts as a sort of feedback on mass loss itself. Namely, a lower value of η would have allowed a slightly larger growth of the luminosity after which, due to the stiff dependence of \dot{M} on L , almost identical conditions as those shown here would have been met. Being $\dot{M} \propto L^{3.7}$, a decrease of η by a factor of ten would only have increased by a factor $\sim 2 \div 2.5$ the total number of pulses for the $6M_{\odot}$ star. At the upper

Fig. 9. Variation with core mass of ${}^7\text{Li}$ (top) ${}^3\text{He}$ (bottom) surface abundances along the evolution of $6M_{\odot}$ models computed with different initial deuterium abundances. The MS track refers to a model computed starting from the main sequence phase. Times for the three models have been normalized in the course of the second dredge-up.

mass limits, intermediate mass stars are not expected to go through more than $\sim 15 \div 20$ TPs with *realistic* mass loss rates, and the number increases roughly $\propto M^{-2}$ down to $\sim 4M_{\odot}$ which, according to the present computations, is the lower limit to get HBB lithium overabundances for a solar chemistry (see later).

7. Dependence on initial deuterium and lithium

After discussing the main effects due to overshooting and mass loss, let us turn to the exploration of the rest of the parameters space. Reaction 3 suggests that Li-production in AGB should be sensitive to the ${}^3\text{He}$ abundance in the envelope. Also, in Sect. 3 we have seen that the amount of ${}^3\text{He}$ at the beginning of the AGB phase somewhat depends on the residual ${}^3\text{He}$ left at the end of the PMS phase due to early D-burning. It is then interesting to check what happens of Li-production if the initial D-abundance is changed.

We then ignored PMS D-burning, simply by running an evolution starting from zero age MS with no ${}^3\text{He}$. As expected, the overall properties of the run are almost identical to those of the reference track. A vanishingly small difference ($< 0.2\%$) in core mass at the beginning of the AGB phase is present, due to a cumulative difference in the efficiency of $p-p$ burning at the border of the convective core during the main sequence phase. Only in AGB, with less ${}^3\text{He}$ available (Fig.9, bottom panel), the track starting from MS begins to show a behavior of its own in terms of lithium abundance (Fig.9, top panel). In fact, during the first pulses, the growth of $\epsilon({}^7\text{Li})$ is slower, and the maximum value –attained after $5 \div 6$ pulses– is ~ 3.7 .

Since the temperature profile within the whole convective region is the same for both the present model and the reference one, we can say that the ${}^3\text{He}$ abundance is the second most important parameter other than T_{bce} influencing lithium production in AGB. This is confirmed by one further run starting from PMS, with an initial D-abundance half of the standard one. As expected, we found an intermediate situation between the two above.

A comment is due to this result. For the test structure, the amount of ${}^3\text{He}$ produced by incomplete $p-p$ chain during the evolutionary phases prior to AGB is about twice the amount due to early D-burning, *with a proto-solar abundance of deuterium*. If (as expected) the cosmological D-abundance was larger than the present one (by a factor of 2 or more, depending on the interpretation

of observations of high redshift absorbers along the lines of sight of distant quasars (Tytler et al. 1996, Songaila et al. 1997), intermediate mass stars of earlier stellar populations must have been more vigorous producers of ${}^7\text{Li}$ than the present ones.

Lastly, also the influence of initial lithium the AGB Li-production was tested. An evolution starting with a lithium abundance of $X({}^7\text{Li}) = 10^{-8}$ was followed. As expected, and in full agreement with Sackmann & Boothroyd (1992), no effect on the final results was found. The structure loses any memory of the previous **history** of lithium at the beginning of the AGB phase, and the lithium abundance during TPs is solely determined by T_{bce} and the ${}^3\text{He}$ abundance.

In summary, the results are independent of the initial lithium abundance, but somewhat sensitive to the initial deuterium abundance, at least during the first TPs. If (as we will see) large mass loss rates can terminate AGB evolution shortly after the ignition of TPs, complete evolutions starting from PMS, with D-burning included, are necessary to correctly evaluate Li-production by intermediate mass stars.

8. Different initial chemistries

To fully exploit Li-production during the life of the Galaxy, it is obviously necessary to compute also AGB models for metal abundances lower than solar. We then followed two more evolutions of $6M_{\odot}$ stars with, respectively, $Y=0.26$, $Z=0.01$ and $Y=0.24$, $Z=0.001$. Some results are shown in Fig.10.

The first effect found was an increase in the core mass at the beginning of the TP phase, when decreasing Z . Most of the effect is due to the larger convective core mass in MS, consistently with the larger MS luminosity. As a consequence, also T_{bce} is larger for lower Z . This leads to a larger consumption of ${}^7\text{Li}$ prior to the AGB phase but, as we have seen before, the evolution of lithium before the Cameron/Fowler mechanism ignites is of no consequences for the following Li-evolution.

In AGB, due both to the larger core mass and to the lower surface opacity, low- Z models have larger values of T_{bce} and larger surface luminosities. This accelerates Li-evolution: the maximum value of $\log \epsilon({}^7\text{Li})$ (~ 4.3 for $Z=0.001$) is reached in a shorter time with respect to the solar case. Of course, also the following evolution (depletion of ${}^3\text{He}$ and of ${}^7\text{Li}$) is accelerated, since T_{bce} overcomes 10^8K . Let us insist that, to study the evolution *as a whole* (i.e.: also when ignoring the details of the surface Li-evolution) of these structures, full coupling between nuclear and turbulent chemical evolution is an absolute prerequisite, since the CNO isotopic concentrations in the convective fraction of the H-burning shell largely determine the nuclear output.

Fig. 10. Variation with time of the surface lithium abundance, luminosity and temperature at the bottom of convection, computed for a $6M_{\odot}$ model with three different metallicities. Lower Z models burn lithium faster due to the larger temperature at the base of the envelope. Computations were made without including mass loss and overshooting.

Fig. 11. The evolution with time of the difference in mass between the H-exhausted and the He-exhausted layers, when asymmetric (dotted line) and symmetric (solid line) overshooting are considered. In the latter case, although the total mass of the He-rich intershell is initially slightly larger, overshooting from the bottom of the convective envelope prevents accumulation of helium and the onset of TPs.

The total duration of an intermediate mass star as a super-lithium rich object is then a strong function of the metallicity: very roughly, $\tau_{\text{Li}} \propto Z^{1/3}$.

9. Overshooting ”from below”

The last test performed on the $6M_{\odot}$ star before going to the discussion of lower mass models is the case in which exponentially decaying diffusive overshooting, fully coupled to nuclear evolution, occurs also *from below* any convective shell/envelope all through stellar evolution. Also in this case, the value of the free parameter ζ has been fixed to 0.02 (*symmetric* overshooting).

A similar framework has been shown by Herwig et al. (1997) to produce third dredge-up and carbon stars for relatively low initial mass structures. Our results for initial masses $M \leq 5M_{\odot}$, which will be discussed in a next paper, are in substantial agreement. Overshooting *from below* leads to the origin of C-stars due to two combined effects:

- during the TP, helium in the He-C-rich convective shell is overshooted to inner regions, where the temperature is larger. Due to the very stiff power dependence of the 3α reactions on T, and to the fact that a relatively large abundance of He is mixed down, the power of the pulse at the peak is largely increased. The feedback of the structure to the larger energy output leads to a deeper sinking of the external convective envelope when the H-shell is turned off, and:
- overshooting from below the envelope as a whole, obviously facilitates the third dredge-up process.

What we examine here is instead likely to be an extreme case, which can be however of interest in the framework of the most luminous, Li-rich AGB stars with little (or no) trace of s-processed elements (see for instance Garcia Lario et al. (1998) in a spectroscopic survey of

IRAS sources selected to probably contain the most massive galactic AGBs).

In Fig.12 we compare the evolution of the $6M_{\odot}$ with core overshooting and mass loss described in Sect. 6, with an analogous evolution including also overshooting *from below* the convective regions (also defined: *symmetric* overshooting case). The two evolutions have been shifted in time such that, at the same moment, in both cases the luminosity contribution from the *thick* He–burning shell following the second dredge up drops to 20% (Fig.6c).

In the case with *symmetric* overshooting, the decline of the efficiency of the He–burning shell preceding the onset of the TP phase is faster than in the *asymmetric* case, ultimately dropping to zero. Of course, in the other case, after a minimum contribution of the He–shell, thermal pulses begin taking place. Let us focus our attention on Fig.11 to understand the reason for the different behaviors.

The two tracks show the thickness in mass of the region between the first grid point in which hydrogen is completely exhausted, and the last grid point where some helium is still present. Then, they do not show the total amount of intershell helium in solar masses. Steps down mark the instant when helium is completely exhausted in the lower grid point in which it was formerly present and, as can be seen, zoning in this region is relatively coarse ($\sim 0.0005M_{\odot}$) since the occurrences there are almost *linear*. The upward slopes following each step down show instead the effect of the outward H–shell shift, with corresponding accumulation of fresh helium in the shell.

The dotted line (*asymmetric* overshooting) shows that, following each step downward, accumulation of new helium is always present (even if the total thickness of the He–rich region decreases). Around $t = 1.7 \cdot 10^4$ years, the accumulation of helium leads to the ignition of the first (still weak) TP. From the solid line (*symmetric* overshooting) we instead see that, in a much earlier phase, downward steps are not followed any more by accumulation of new helium. On the contrary, approximately when the TPs should begin, the thickness of the He–rich region begins to drop fast.

This is the consequence of overshooting *from below*. Soon after the ignition of the H–burning shell, this latter begins being fully penetrated by overshooting, ultimately leaking through the whole shell and into the H–exhausted (and C–enriched) mantle below. At this point, all the helium produced by H–burning is mixed up in the envelope, and even some helium (and carbon) from the He–mantle are mixed up. Lack of accumulation of helium leads to the impossibility of igniting TPs, and the star goes on stationarily losing mass in conditions of HBB (and then of Li–overabundance, but with little surface carbon, which is almost entirely transformed into N^{14} by the CNO cycle). Ultimately, when the He–mantle is almost completely destroyed, the large abundances of C^{12} leaked by overshooting and convected inside the furiously CNO burning

H–shell cause a fast increase in surface luminosity (and mass loss) terminating the AGB phase.

Let us insist on the requirement of a full–coupling between mixing and nuclear evolution, especially in these phases. More than this, the diffusion coefficient must be *physically sound*, since the evolution of the H–shell is largely sensitive to the velocity with which fresh C^{12} from below is convected outwards. Now, if there is agreement on something among MLT users, it is clear that MLT is unable to correctly predict mixing timescales at the base of an AGB envelope (Wagenhuber & Groenewegen 1998). The FST convective model, on the contrary, is not bound to unphysically large scale length, and also predicts more sound convective velocities, since the turbulent fluxes are far more consistent with experimental ones. It is then unlikely that such extreme conditions could be investigated with descriptions of turbulence and mixing different from the present ones. This is also true of the first–order expansion of the nuclear evolution as a whole (Arnett & Truran), since in thin shell conditions one can easily get (relatively) large values of ΔX , and a zero–order evolutionary scheme would badly overestimate H–consumption.

9.1. Possible evolutionary consequences

Figures 13 show two models in the latest phase of this evolution: comparison shows how the hydrogen shell *penetrates* into the structure, dredging up the top of the carbon core. Notice that this kind of evolution *completely wipes out the helium buffer layer*. So, we ultimately expect a (massive) white dwarf showing carbon and even oxygen in large quantities up to the stellar surface, below a very thin H–rich layer (if any).

This is just the structure *ad hoc* hypothesized in hydrodynamic theoretical models to explain the *fast nova* mechanism (e.g. Prialnik & Kovetz 1984, Kutter & Sparks 1989), and actually seen in nova ejecta (Williams 1985, Truran & Livio 1986). In fact, not only large masses (i.e. surface gravities) are required, but the short evolutionary times (hours) do not allow the *complete* CNO cycle to operate, because of the bottleneck of the ^{13}N decay, which takes ~ 10 min. So, only the energetics of the $^{12}C + p$ reaction is available, and the observed energy outputs (and chemical ejecta) are consistent with large overabundances of ^{12}C , about $20 \div 40\%$ by mass. In the presence of an He–intershell, hardly the H–rich matter accreted to the surface could be able to mix with the C–O rich core. In the present framework, instead, *symmetric* overshooting and consequent shortage of the He–intershell just for the more massive pre–WDs spontaneously leads to the conditions in which *fast novae* would **occur**.

This may be also the evolutionary path which finally leads to the observed surface chemical abundances of some members of the PG1159 class of hot white dwarfs, including their prototype. In fact, Werner et al. (1991) have found significant overabundances of carbon and oxygen in

Fig. 12. Comparison between the $6M_{\odot}$ evolution including core overshooting and mass loss (dashed) and the evolution including ‘symmetric’ overshooting. In this latter case, no TPs are present due to penetration of overshooting in the He-rich intershell.

their spectra, and models of nonadiabatic pulsations of PG type stars require a large Oxygen and Carbon overabundances just below the photosphere to drive the pulsational instabilities (Stanghellini et al. 1991).

Notice, in passing, the presence of a ^{13}C pocket just below the H/C interface, due to the leakage of protons in the C-rich layers. In principle, ^{13}C could act as a neutron source to build up s-process elements (e.g. Iben 1982), but it must be recalled that TPs are not present in this case. So, the temperature of the ^{13}C -rich layers is never larger than $100 \div 120$ MK, and s-processes operate at a very slow pace.

In summary, according to the above described framework, a possible observational signature of the presence of overshooting *from below* the convective envelope could arise from:

- the practical impossibility of getting a different, straightforward evolutionary scenario giving rise to low-mass (and low-luminosity) carbon stars (Herwig et al. 1997);
- the observation that the most massive AGB stars in the Galaxy, selected as those already having a circumstellar envelope due to mass loss, clearly show a surface chemistry due to HBB, but no track of s-processed elements (Garcia Lario et al. 1999);
- the anomalous overabundances of C and O in some PG1159 WDs and, related to this feature:
- the straightforward explanation of the surface exposure of C/O mixtures in large mass WDs required to explain the fast nova mechanism.

Of course, other explanations are possible for all the above features. For instance, the lack of s-process enhancements in the Garcia Lario et al. sample may be due to the fact that pollution of the massive envelope of a massive AGB stars by s-processes would require a long series of TPs, while lithium production occurs as soon as the star is on the AGB. What is relevant is, in our opinion, the fact that several, still *qualitatively* (and not only *quantitatively*) unexplained, features, spontaneously **occur** if *symmetric* overshooting is allowed.

10. Mass dependence

In the end, we also computed evolutionary sequences for different initial mass stars, starting from $3.5M_{\odot}$ and with steps of $0.5M_{\odot}$. The chemistry was solar, and both overshooting *from above* and mass loss (respectively: with $\zeta = 0.02$ and $\eta = 0.1$) were included. Of course, these computations are still preliminary to a full investigation

Fig. 15. For different total masses and models having $Z=0.02$ and core overshooting we show the variation with time of the lithium abundance, total luminosity and T_{bce} .

on lithium enrichment of the interstellar medium from intermediate mass AGB stars.

The model of $3.5M_{\odot}$ never reaches HBB conditions, and the Cameron-Fowler mechanism is then not ignited. Also, the same model does not undergo the second dredge-up, by a small amount. Already at $4.0M_{\odot}$, both second dredge-up and HBB are found if overshooting is included, whereas sequences without overshooting show these features only from $4.5M_{\odot}$ on. In all the investigated cases, a strict relation was found between the presence of second dredge-up, and the following onset of HBB conditions.

Broadly speaking, in all the mass range for which HBB is found, the evolution follows similar paths at a lower pace the lower is the mass. Also the amplitudes of the various features connected with HBB (Li-overabundance, fast increase in luminosity at the beginning of the AGB phase etc.) increase when increasing the total mass, as one could have expected (Fig. 15). A capillary analysis of the details of the various evolutions is then useless, and only the overall results of computations of narrower grids of models, with different masses and chemistries, and with a more realistic mass loss free parameter ($\eta = 0.01 \div 0.02$) will be given in a next paper, as an input for galactic evolution models.

One last result is instead worth showing. When in AGB, the evolution tends to become *chaotic* in the sense that stars of different masses, evolutionary phases and pulse/interpulse phases share the same region of the HR diagram. However, some *attractors* can be still identified, as longer lasting phases. Fig. 16 shows, in the lithium vs. luminosity plane, what could be expected from our theoretical evolutionary paths of $4.0 \div 6.0M_{\odot}$ stars, with (asymmetric) overshooting and mass loss ($\eta = 0.1$). A mass function $\propto M^{-2}$ has been assumed, and a handful of points have been spread along the tracks, randomly selected linearly with time, starting from the beginning of AGB.

Also, a sample of observed stars in the Magellanic Clouds (Smith et al. 1995) are shown in the same figure. Although the metal abundances of these latter are lower than the theoretical ones, one can identify some first correspondences. Observed stars of low luminosity are likely to be still lithium undepleted. The theoretical points mark quite well the left-upper envelope of the observations. More than that, we have to recall that the present evolutionary tracks have been followed for a low number of

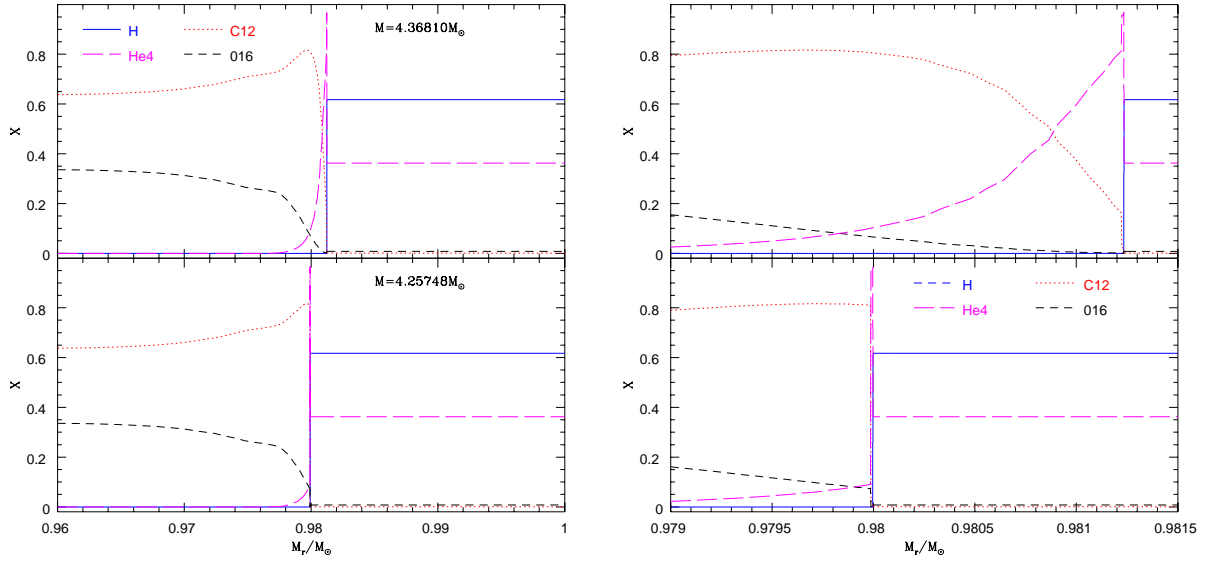


Fig. 13. We show the chemistry of two models of $6M_{\odot}$ in late evolutionary phases, when "symmetric" overshooting is present. The right figures are blow-up of the left ones close to the H-burning shell. The dredge-up of carbon and oxygen rich matter from the core to the surface due to penetration of the external convective envelope through the H-rich shell is evident.

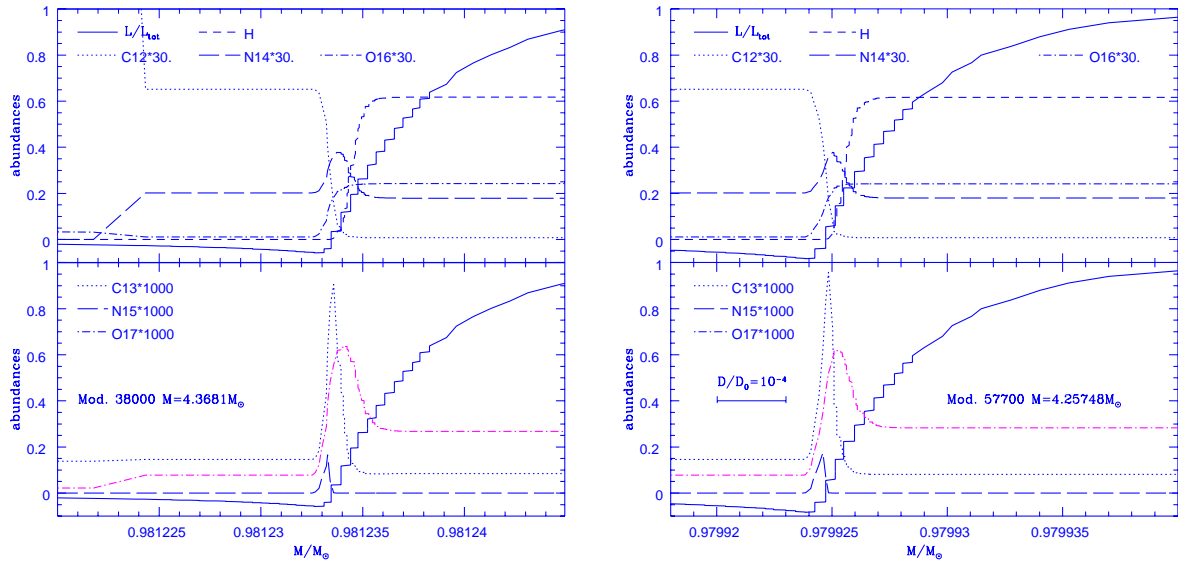


Fig. 14. The same as in Fig.13, but further blown up around the H-burning shell, defined according to the luminosity profile. The hydrogen profile (dashed) shows that convection is able to homogenize the shell almost down to its bottom. The CNO elements show however profiles of abundances *inside* the convectively mixed region, which can only be obtained by solving the coupled diffusive and nuclear evolution. The importance of applying this latter algorithm could not be better clarified.

TPs, and that models show a trend, when going on with the evolution, to decrease both the surface lithium abundances and luminosities. In other words, more complete tracks up to planetary nebula ejection would have led to populate also the region where the most of the observed

stars are present, as also suggested by the *turn-downs* already visible in the upper part of the theoretical distributions

Of course, no firm conclusions can be still established by these first results, also because the observational error

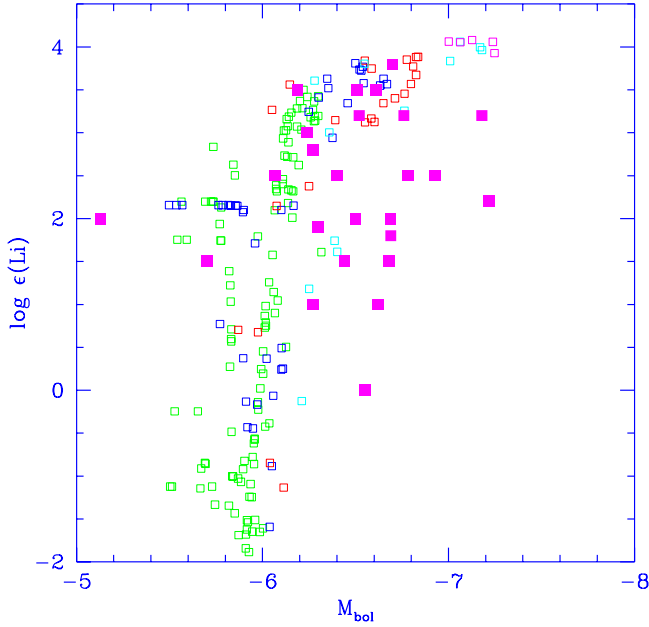


Fig. 16. Theoretical positions (open squares) in the lithium vs. luminosity plane for the 4.0, 4.5, 5.0, 5.5 and 6.0 M_{\odot} models of solar chemistry with (asymmetric) overshooting and mass loss. Also observed stars in the magellanic clouds (full squares) are shown.

boxes are quite large, and a selection effect is certainly present, being easier to detect lithium in the more luminous objects. However, more extended evolutionary tracks with the correct chemical inputs (in progress of computation) will probably strengthen the overall agreement between the theoretical and experimental framework.

11. Conclusions

We have examined the details of lithium production in intermediate mass stars of solar metallicity during the AGB phase. Lithium is naturally produced in FST models including core overshooting for masses $M \gtrsim 4M_{\odot}$, and $\gtrsim 4.5M_{\odot}$ without overshooting. In MLT models, at least $6M_{\odot}$ are instead required to ignite HBB with a solar tuning of α , if core overshooting is not allowed. These structures are so largely dependent on convection, due to the leakage of the convective envelope in the H-burning shell, that also other differences (for instance in the mass – luminosity relation etc.) between MLT and FST structures are striking enough that careful comparisons between models and observations could help constraining the convection model.

The amount of lithium produced during the AGB phase is independent of the assumed initial lithium abundance, while it is somewhat dependent on the initial deuterium, and on PMS evolution.

Core overshooting during MS H-burning, leading to larger core masses and luminosities in AGB, also affects lithium production, which attains a maximum shortly after the second dredge up. If also overshooting from below the convective envelope is allowed, in the case of the $6M_{\odot}$ star we find total suppression of the thermal pulses. This mechanism could be responsible for the presence of high luminosity AGB stars with large lithium overabundances, but completely lacking the s-elements enhancement associated to the third dredge-up phase following TPs.

References

- Alexander D.R., Ferguson J.W., 1994, *ApJ* 437, 879
 Arnett W.D., Truran J.W. 1969, *ApJ* 157, 359
 Balachandran S., Lambert D.L., Stauffer J.R., 1988, *ApJ* 333, 267
 Balachandran S., Lambert D.L., Stauffer J.R., 1996, *ApJ* 470, 1243
 Basu S. 1997, *MNRAS* 288, 572
 Bonifacio P., Molaro, P. 1997, *MNRAS* 285, 847
 Blöcker T., 1995, *A&A* 297, 727
 Cameron A.G., Fowler W.A., 1971, *ApJ* 164, 111
 Canuto V.M., Mazzitelli I., 1991, *ApJ* 370, 295
 Canuto V.M., Mazzitelli I., 1992, *ApJ* 389, 724
 Canuto V.M., Goldman I., Mazzitelli I., 1996, *ApJ* 473, 550
 Caughlan G.R., Fowler W.A., 1988, *Atomic data Nucl. Tab.* 40, 283
 D'Antona F., Matteucci, F., 1991, *A&A*, 248, 72
 D'Antona F., Mazzitelli I., 1996, *ApJ* 470, 1093
 García-Lario P., D'Antona F., Lub J., Plez B., Habing H. 1999, in *IAU Symposium 191 "Asymptotic Giant Branch Stars"*, in press
 Graboske H.C., De Witt H.E., Grossman A.S., Cooper M.S., 1973, *ApJ* 181, 457
 Herwig F., Blöcker T., Schönberner D., El Eid M., 1997, *A&A* 324, L81
 Iben I. Jr. 1982, *ApJ*, 260, 821
 Itoh N., Kohyama Y., 1993, *ApJ* 404, 268
 Itoh N., Mutoh H., Hikita A., Kohyama Y., 1992, *ApJ* 395, 622
 Kutter G.S., Sparks W.M. 1989, *ApJ* 340, 985
 Maeder A., Meynet G., 1991, *A&AS* 89, 451
 Matteucci F., D'Antona F., Timmes F.K., 1995, *A&A* 303, 460
 Mihalas D., Dappen W., Hummer D.G., 1988, *ApJ* 331, 815
 Prialnik, D., Kovetz, A. 1984, *ApJ*, 281, 367
 Rogers F.J., Iglesias C.A., 1993, *ApJ* 412, 572
 Rogers F.J., Swenson F.J., Iglesias C.A., 1996, *ApJ* 456, 902
 Sackmann I.J., Boothroyd A.I., 1992, *ApJ* 392, L71
 Sackmann I.J., Boothroyd A.I., 1995, *Mem.Soc. Astr.It.* 66, n.2, 403
 Sackmann I.J., Smith R.L., Despain K.H., 1974, *ApJ* 187, 555
 Scalo J.M., Despain K.H., Ulrich R.K., 1975, *ApJ* 196, 805
 Smith V.V., Lambert D.L., 1989, *ApJ* 345, L75
 Smith V.V., Lambert D.L., 1990, *ApJ* 361, L69
 Smith V.V., Plez, B., Lambert D.L., 1995, *ApJ*, 441, 735
 Soderblom D.R., Oey M.S., Johnson D.R.H., Stone R.P.S., 1990, *AJ* 99, 595
 Soderblom D.R., Jones B.F., Balachandran S., et al., 1993a, *AJ* 106, 1059
 Soderblom D.R., Fedele S.B., Jones B.F., Stauffer J.R., Prosser C.F., 1993b, *AJ* 106, 1080

- Songaila A., Wampler E.J., Cowie L.L. 1997, Nat 385, 137
Spite F., Spite M., 1993, A&A 279, L9
Stothers R.B., Chin C.W., 1992, ApJ 390, 136
Stanghellini, L., Cox, A.N., Starrfield, S. 1991, ApJ, 383, 766
Truran J.W., Livio M. 1986, ApJ 308, 721
Tytler D., Fan X.-M., Burles S. 1996, Nat 381, 207
Ventura P., Zeppieri A., Mazzitelli I., D'Antona F., 1998, A&A
334, 953
Vitense E., 1953, Zs. Ap. 32, 135
Wagenhuber J., Groenewegen M.A.T., 1998, A&A 340, 183
Werner K., Heber U., Hunger, K. 1991, A&A 244, 437
Williams, R.E. 1985, in "Production and distribution of CNO
elements", ed. I.J. Danziger (Garching:ESO), p. 225
Xiong D.R. 1985, A&A 150, 133

This figure "fig1.jpg" is available in "jpg" format from:

<http://arxiv.org/ps/astro-ph/9907245v1>

This figure "fig3a.jpg" is available in "jpg" format from:

<http://arxiv.org/ps/astro-ph/9907245v1>

This figure "fig3b.jpg" is available in "jpg" format from:

<http://arxiv.org/ps/astro-ph/9907245v1>

This figure "fig6a.jpg" is available in "jpg" format from:

<http://arxiv.org/ps/astro-ph/9907245v1>

This figure "fig6b.jpg" is available in "jpg" format from:

<http://arxiv.org/ps/astro-ph/9907245v1>

This figure "fig6c.jpg" is available in "jpg" format from:

<http://arxiv.org/ps/astro-ph/9907245v1>

This figure "fig7.jpg" is available in "jpg" format from:

<http://arxiv.org/ps/astro-ph/9907245v1>

This figure "fig8.jpg" is available in "jpg" format from:

<http://arxiv.org/ps/astro-ph/9907245v1>

This figure "fig9.jpg" is available in "jpg" format from:

<http://arxiv.org/ps/astro-ph/9907245v1>

This figure "fig10.jpg" is available in "jpg" format from:

<http://arxiv.org/ps/astro-ph/9907245v1>

This figure "fig11.jpg" is available in "jpg" format from:

<http://arxiv.org/ps/astro-ph/9907245v1>

This figure "fig12a.jpg" is available in "jpg" format from:

<http://arxiv.org/ps/astro-ph/9907245v1>

This figure "fig12b.jpg" is available in "jpg" format from:

<http://arxiv.org/ps/astro-ph/9907245v1>

This figure "fig15.jpg" is available in "jpg" format from:

<http://arxiv.org/ps/astro-ph/9907245v1>